Conductor Loss in Superconducting Planar Structures: Calculations and Measurements

James C. Booth, *Member, IEEE,* and Christopher L. Holloway, *Member, IEEE*

***Abstract*—We present closed-form expressions of the attenuation constant due to conductor loss for superconducting coplanar waveguide and microstrip transmission lines. These expressions, valid for arbitrary conductor thickness, make use of a numerically determined quantity (the stopping distance Δ) that depends on the material properties and edge shape of the superconducting transmission line. Once Δ is determined, the attenuation constant for any planar geometry can be obtained without further numerical calculation, making this technique attractive for use in the design of circuits incorporating superconducting planar elements. The results of this calculation compare favorably with full numerical calculations and also with experimental data on high-temperature superconducting coplanar transmission lines, illustrating the accuracy and applicability of the calculation for determining the conductor loss of superconducting circuit elements.**

***Index Terms*—Attenuation, coplanar transmission lines, high-temperature superconductors, microstrip, superconducting microwave devices.**

I. Introduction

HIGH-TEMPERATURE superconducting (HTS) materials are being increasingly used in high- performance passive microwave applications [1], such as filters for wireless communications, due in part to the fact that the quality of HTS thin films has greatly improved in recent years. Since these materials are readily available in thin-film form, many superconducting microwave elements are being implemented in planar geometries such as microstrip and coplanar. It is, therefore, increasingly important to be able to accurately model the critical parameters of superconducting coplanar and microstrip structures, in order to facilitate the design and fabrication of high-performance superconducting microwave components.

To calculate the conductor loss in planar microwave circuits, various techniques can be used, from full numerical calculations to quasi-analytical methods such as Wheeler's rule. While numerical techniques are capable of very high accuracy, they are computationally intensive and often difficult to use and, hence, do not lend themselves to ready use in design. Instead, closed-form expressions for the conductor loss are desirable for this purpose and can be obtained using Wheeler's rule. However, if the ratio t/δ (where δ is the relevant skin depth and t is the thickness of the conductor) is small or comparable to unity, then Wheeler's rule breaks down and gives unreliable results. The failure of analytical methods for thin films can be a serious limitation for the design and modeling of planar structures, particularly for superconducting elements, where the film thickness is often comparable to the relevant penetration depth.

In this paper, we present closed-form expressions for the attenuation constant due to conductor loss of superconducting coplanar waveguide (CPW) and microstrip transmission lines; expressions which are valid for any conductor thickness. Analogous expressions for the phase constant will be presented in future work. The calculation makes use of a numerically determined quantity (the stopping distance Δ) that depends on the material properties and shape of the superconducting transmission line. Once determined, the stopping distance is used in an analytical expression for the attenuation due to conductor loss for any transmission-line geometry and film thickness. No further numerical calculations are necessary once Δ has been obtained, making this approach well suited for use in the design of practical superconducting circuit elements.

In what follows, we first describe the numerical determination of the stopping distance for different material parameters and then present the analytical expressions for the attenuation constant for CPW and microstrip geometries. The results of the calculations are then compared with full numerical simulations of the superconducting attenuation constant found in the literature. A detailed comparison of the calculation with experimental data for high-T_c superconducting CPW transmission lines and resonators of different geometries, measured using a cryogenic microwave probe station, is then presented. Comparisons are also made between normal metal conductors and superconductors in the microstrip geometry. We conclude with a discussion of the limitations of this approach for the calculation of the conductor loss in superconducting planar circuits.

II. Determination of the Attenuation Constant

To arrive at a closed-form expression for the conductor loss valid for arbitrary thickness conductors, it is tempting to apply standard perturbation methods. An approximate current density on the strips can be obtained by assuming the conductors are infinitely thin, and this current density can then be used in the expression for the attenuation constant

$$\alpha \approx \frac{R_s}{2Z_0} \int_{\text{top,bottom}} \left(\frac{J}{I}\right)^2 dl. \tag{1}$$

where the integral is carried over both the top and bottom portions of the strip conductor. Here, J is the approximate current

Manuscript received February 13, 1998. The work of J. C. Booth was supported under a National Institute of Standards and Technology/National Research Council post-doctoral research associateship.

J. C. Booth is with the National Institute of Standards and Technology, Boulder, CO 80303 USA.

C. L. Holloway is with the Institute for Telecommunication Sciences/NTIA, Boulder, CO 80303 USA.

Publisher Item Identifier S 0018-9480(99)04285-4.

density on the strip, I is the total current on the conductors, R_s is the surface resistance of the strip conductors, and Z_0 is the characteristic impedance of the structure. However, because the current density on an infinitely thin perfectly conducting strip diverges as $1/\sqrt{r}$ (where r is the distance from the nearest edge), the integration of $|J|^2$ in (1) diverges logarithmically, giving no useful results for the conductor loss.

To avoid this difficulty, Lewin [2], Vainshtein and Zhurav [3], and Holloway and Kuester [4], [5] have developed an alternative approach, in which the conductor loss is approximated by carrying out the integration in (1) not to the strip edges, but to some finite distance, the stopping distance Δ, away from the edges of the strip. The value of Δ is determined numerically and is a function only of the local edge geometry: the strip thickness, shape of the edge, and material of the strip conductor. The stopping distance and resulting expressions for the normal metal conductor loss for CPW and microstrip lines are presented by Holloway and Kuester [4], [5].

To determine the conductor loss for superconducting planar structures, a new stopping distance Δ must be calculated. This is accomplished in a manner analogous to the normal metal case by noting that the power loss in the region local to the edge of a superconducting strip can be accurately determined using an asymptotic solution for the fields near the isolated edge [4]. The stopping distance Δ can then be found by equating this power loss to the power loss found from the stopping-distance method using the current distribution of a zero-thickness perfect conductor. To describe the electrodynamic response of a superconductor, one can, in general, define a complex conductivity $\tilde{\sigma} = \sigma_1 - i\sigma_2$, where the real (imaginary) part of the conductivity describes the response of the normal (super) fluid in a two-fluid picture [6]. These two components of the conductivity can be written conveniently in terms of a superconducting magnetic penetration depth $\lambda = \sqrt{1/\mu_0\omega\sigma_2}$ and a normal fluid skin depth $\delta_{\rm nf} = \sqrt{2/\mu_0\omega\sigma_1}$. The resulting stopping distance for a superconductor as a function of the material properties (the strip thickness t, normal fluid skin depth $\delta_{\rm nf}$, and magnetic penetration depth λ) is shown in Fig. 1 (for a 90° edge profile); it can be subsequently used to obtain the conductor loss for planar superconducting structures. Note that the stopping distance Δ depends sensitively on the ratio $t/2\lambda$, but is relatively insensitive to the ratio $t/2\delta_{\rm nf}$, provided that $\lambda \ll \delta_{\rm nf}$ (which implies that the material responds as a good superconductor).

Once the stopping distance Δ has been determined, the attenuation constant for a superconducting CPW transmission line of dimensions a, b (see Fig. 2 inset) can be simply calculated from the expression [5]

$$\alpha \approx \frac{R_{sm} b^2}{16 Z_0 K^2(a/b)(b^2-a^2)} \cdot \left\{ \frac{1}{a} \ln\left(\frac{2a(b-a)}{\Delta(b+a)}\right) + \frac{1}{b} \ln\left(\frac{2b(b-a)}{\Delta(b+a)}\right) \right\} \quad (2)$$

where $K(a/b)$ is the elliptic integral of the first kind and

$$R_{sm} = \mu_0 \omega t \, \mathrm{Im}\left(\frac{\cot(k_c t) + \csc(k_c t)}{k_c t}\right) \quad (3)$$

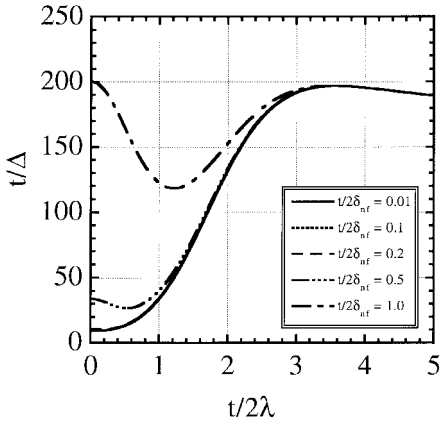

Fig. 1. Stopping distance Δ plotted as t/Δ as a function of $t/2\lambda$ for various values of $t/2\delta_{\rm nf}$.

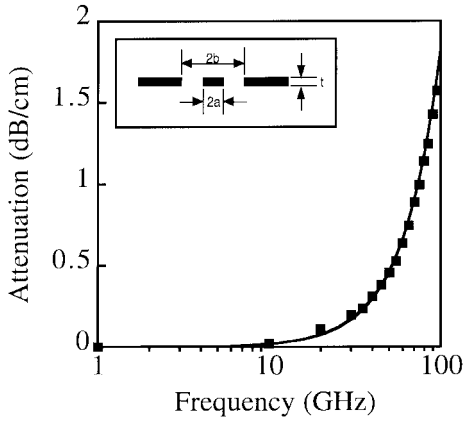

Fig. 2. Attenuation constant versus frequency for a CPW transmission line calculated by the mode-matching technique [8] (squares) and using (2) (solid line). Inset: CPW geometry in cross section.

is a modified surface impedance for a superconductor strip of thickness t. Here, k_c is the (complex) wavenumber in the superconductor at a frequency ω given by [6]

$$k_c^2 = \left(\frac{1}{\lambda}\right)^2 + 2i\left(\frac{1}{\delta_{\rm nf}}\right)^2. \quad (4)$$

The expression in (2) includes the loss due to the signal line and both ground planes and also assumes that the ground-plane width is large compared with the strip width $(2a)$ or the gap spacing $(b-a)$.

For a microstrip line of width W, the corresponding expression for the attenuation constant is [4]

$$\alpha \approx \frac{R_{sm}}{2\pi^2 Z_0} \frac{\ln\left(\frac{W}{\Delta} - 1\right)}{W}. \quad (5)$$

Equation (5) corresponds to the loss of only the strip portion of the microstrip line. For some microstrip geometries, the conductor loss associated with the ground plane may become comparable to the loss of the strip [4] and must be taken into account in order to accurately calculate the total conductor loss of a microstrip line. Expanding on previous work [7], we

approximate the conductor loss of the ground plane by

$$\alpha_{\rm gr} \approx \frac{R_{sm}}{Z_0 \pi W}\left\{\tan^{-1}\left(\frac{W}{2h}\right) - \frac{h}{W}\ \ln\left[1+\left(\frac{W}{2h}\right)^2\right]\right\}. \tag{6}$$

In this expression, h is the distance from the center line to the ground plane, and the thickness of the ground plane is used in the calculation of R_{sm} in (3).

With Δ, determined from Fig. 1 for the appropriate material properties, (2) and (5) can be readily used to calculate the loss for finite-thickness CPW or microstrip structures of any geometry, with no further numerical calculations. However, one must use caution if interpolation between curves of constant $t/2\delta$ in Fig. 1 is used in order to obtain a more accurate value for t/Δ. In earlier work [4], t/Δ was plotted as a function of $t/2\delta$ for the case of a normal metal conductor ($t/2\lambda = 0$ in Fig. 1). Such a plot shows that t/Δ is a *nonmonotonic* function of $t/2\delta$ for values of $t/\delta > 1$. This implies that interpolation between curves in Fig. 1 may not always provide a correct value for t/Δ. However, as we show below, most good superconductors are described adequately by the curves presented without the need to interpolate between them.

III. Comparison with Numerical Calculations

To verify the validity of our approach, we show, in Fig. 2, a comparison of the attenuation constant calculated from (2) with numerical results from the mode-matching calculation of Heinrich [8] for a superconducting CPW line of thickness $t = 0.3$ μm and with $a = 7.5$ μm and $b = 17.5$ μm over the frequency range 1–100 GHz. The material properties of the superconductor are given by a London penetration depth of $\lambda = 300$ nm and a normal fluid conductivity of $\sigma_1 = 8.2 \times 10^5$ S/m. These material parameters are typical for HTS materials at 77 K. With this value for σ_1, the quantity $t/2\delta_{\rm nf}$ ranges from 8.5×10^{-3} to 8.5×10^{-2} over the frequency range 1–100 GHz. Fig. 1 shows that Δ is effectively independent of the value of $\delta_{\rm nf}$ over this entire frequency range, implying that a single value of Δ is sufficient for a complete description of the superconductor in this example. The excellent agreement between the full numerical simulation of Heinrich and the present calculation illustrates the accuracy of our calculation, specifically for a range of materials parameters representative of high-T_c superconductors.

IV. Comparison with Experimental Data

In order to further demonstrate the validity of our calculation and to illustrate its application, we compare the results of (2) to experimental data on actual superconducting CPW transmission lines and resonators fabricated from $YBa_2Cu_3O_{7-\delta}$ (YBCO) thin films (with critical temperatures of $T_c \approx 91$ K) grown by pulsed-laser deposition on $LaAlO_3$ substrates. Before the thin films are patterned into coplanar structures, the surface impedance of the superconducting samples is measured as a function of temperature using a sapphire dielectric resonator [9], giving quantitative values for the material properties of the superconducting thin films. Our CPW structures are subsequently patterned from these same films by optical photolithography and Ar ion milling. Gold contact pads are evaporated onto the CPW devices to facilitate reproducible electrical contact.

The patterned CPW transmission lines and resonators are measured at temperatures below T_c using a low-temperature microwave probe station [10]. The probe station incorporates movable air coplanar probes that are cooled to cryogenic temperatures under vacuum along with the superconducting samples. This allows many different superconducting devices, which are often patterned onto a single thin film, to be characterized rapidly during a single cooldown. Two different measurement techniques are used: transmission-line measurements and resonator measurements. For characterization of the transmission lines, a low-temperature on-wafer calibration scheme [11] is used to obtain the attenuation constant as a function of frequency from 50 MHz to 40 GHz. The errors associated with the attenuation-constant determination are primarily due to the precision with which the transmission coefficient can be reproducibly measured, which is probably limited in the current measurements by irreproducible contact and temperature drift during the measurements. For structures which have very low losses, resonator meausurements become necessary as the attenuation constant becomes smaller than the resolution limit of the transmission measurements. For these measurements, the movable probes are decoupled from the transmission-line structures, creating a resonant structure. The quality factor of the fundamental resonance and several overtone resonances are then measured. Although the resonant measurements are much more sensitive than the transmission measurements described above, data is obtained only at discrete frequency points. In addition, as the conductor losses decrease, contributions to the measured quality factor due to dielectric loss in the substrate and radiation losses become increasingly important. For the measurements presented here, the quality factor appears to be dominated by conductor losses. The results of these different measurements can then be directly compared to the response calculated from (2) for a number of different CPW geometries.

Fig. 3 shows the measured attenuation constant at 76 K for three CPW transmission lines of three different geometries fabricated from the same YBCO film of 50-nm thickness. The center conductor linewidths of the different transmission lines are: 1) 21 μm; 2) 53 μm; and 3) 105 μm, and the gap spacing between the center conductor and ground planes is varied to maintain 50-Ω characteristic impedance. Also shown in Fig. 3 are the results of (2), using values for $\sigma_1 = 1.72 \times 10^6$ S/m, and $\lambda = 316$ nm. Both σ_1 and λ are extracted from the dielectric-resonator measurements of the surface impedance of the thin films at $T = 76$ K. In order to determine the absolute value for the penetration depth λ, we combine our dielectric resonator measurements, which yield $\Delta\lambda(T)$ from the resonant frequency shift, with results for the absolute value of the penetration depth $\lambda(T = T_{\rm low})$ obtained from mutual inductance measurements of similar samples [12], [13]. The calculation results obtained in Fig. 3, therefore, make use of no adjustable material parameters and yield results that agree

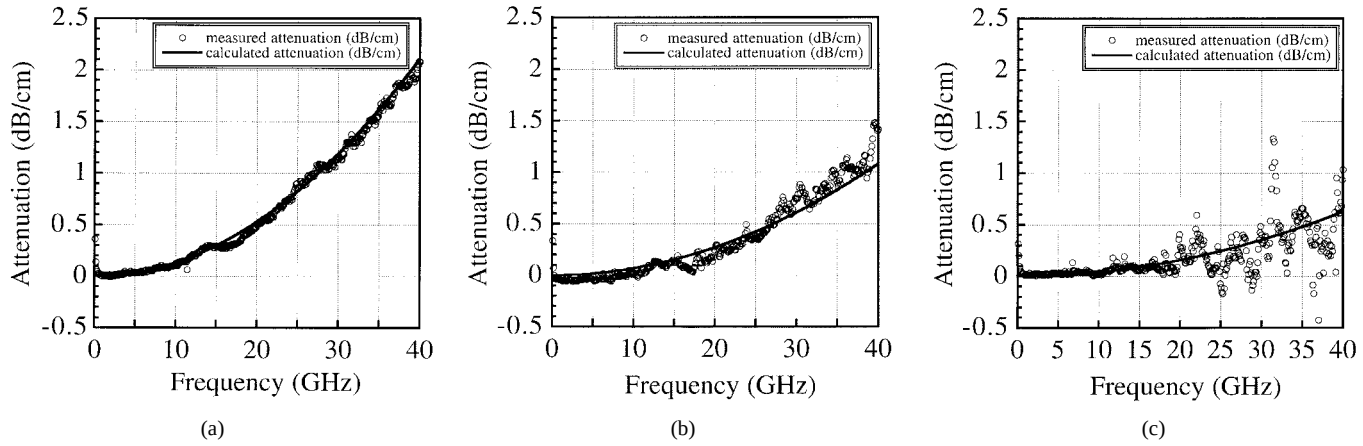

Fig. 3. Attenuation constant versus frequency at $T = 76$ K for three different CPW transmission lines fabricated from a single YBCO thin film. Also shown is the attenuation constant calculated for each geometry with $t = 50$ nm, $\lambda = 316$ nm, and $\sigma_1 = 1.72 \times 10^6$ S/m. The transmission line geometries are given by: (a) $a = 10.5$ μm, $b = 50.5$ μm, (b) $a = 26.5$ μm, $b = 127.5$ μm, and (c) $a = 52.5$ μm, $b = 252.5$ μm.

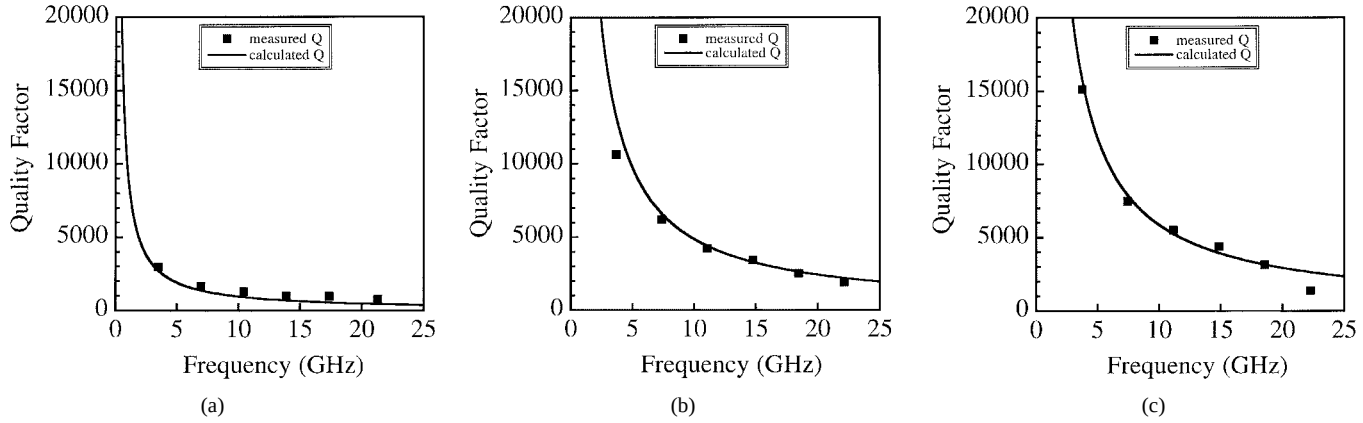

Fig. 4. Measured quality factor versus frequency at $T = 30$ K for 9.85-mm-long CPW resonators fabricated from three different thickness YBCO thin films. Also shown is the quality factor calculated for each transmission line using $a = 10.5$ μm and $b = 50.5$ μm. The material properties are given by: (a) $t = 50$ nm, $\lambda = 205$ nm, $\sigma_1 = \sigma_1 = 2.13 \times 10^6$ S/m, (b) $t = 320$ nm, $\lambda = 205$ nm, $\sigma_1 = 2.63 \times 10^6$ S/m, and (c) $t = 500$ nm, $\lambda = 205$ nm, $\sigma_1 = 3.13 \times 10^6$ S/m.

very well with the measured experimental data for all three different transmission-line geometries.

The experimental data in Fig. 3 are obtained in a region where Δ is nearly independent of material parameters $(t/\lambda \ll 1)$. We can obtain further confirmation of our calculations by using material parameters such that $t/\lambda \approx 1$. Such data are obtained using CPW resonators fabricated from thicker films and measured at low temperatures where the penetration depth λ is smallest. Fig. 4 shows the quality factors of CPW resonators of center linewidth 21 μm measured at 30 K for film thicknesses: 1) 50 nm; 2) 320 nm; and 3) 500 nm. Resonator measurements for these samples are necessary because the attenuation constant has become smaller than the sensitivity limit of our calibrated transmission-line measurements over a large portion of the measurable frequency range. Fig. 4 also shows results of our calculation for the resonator quality factor based on material parameters obtained from our dielectric-resonator measurements, as described previously. For this example, the quantity t/λ varies in the 0.24–2.4 range. Since the quality factor Q is given by $Q = \beta/2\alpha$, where β and α are the phase and attenuation constants, respectively, we need an expression for β in order to obtain the calculated Q from our calculated attenuation constant. For the data in Fig. 4, we use the approximation $\beta \approx \omega/c\sqrt{\varepsilon_{\text{eff}}}$ (where c is the speed of light, and ε_{eff} is the effective dielectric constant, related to the substrate dielectric constant ε_{sub} for the coplanar geometry by $\varepsilon_{\text{eff}} = (\varepsilon_{\text{sub}} + 1)/2$. Using $\varepsilon_{\text{sub}} = 24$ for the dielectric constant of $LaAlO_3$, this gives $Q = (3.216)f/\alpha$, where f is the frequency in gigahertz and α is in decibels/centimeter.

The above approximation ignores the kinetic inductance of the superconducting thin film. However, calculations of the kinetic inductance [14] show that this contribution is less than 8% for the 50-nm films, which have the largest kinetic-inductance contribution of the three measured samples. Therefore, the calculated Q in Fig. 4 slightly underestimates the actual value for the quality factor and is more accurate for the thicker films. Nonetheless, this comparison shows that the calculation also agrees well with experimental data in the regime where $t/\lambda \approx 1$. These comparisons to experimental data on actual HTS circuits demonstrate the applicability of our calculation for a wide range of materials parameters appropriate to the HTS materials.

In order to demonstrate the application of these results to geometries other than coplanar, we present in Fig. 5 calculations of the attenuation constant of a microstrip transmission

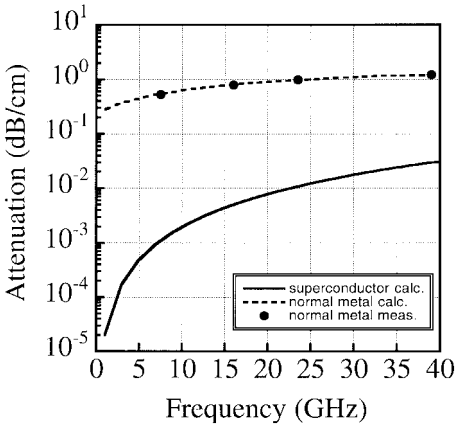

Fig. 5. Attenuation constant for a microstrip transmission line, calculated for the case of a normal metal conductor and superconductor. Also shown are the experimental data of Goldfarb and Platzker [15]. For this example, the geometry is given by the following: center conductor width = 20 μm, distance to ground plane = 100 μm, thickness = 3 μm, and relative dielectric constant of substrate = 12.9. For the normal conductor case, the conductivity is given by $\sigma = 4.1 \times 10^7$ S/m and for the superconductor case , the material properties are described by a penetration depth of $\lambda = 300$ nm and a normal fluid conductivity of $\sigma_1 = 8.2 \times 10^5$ S/m.

line for both a normal metal conductor and a superconductor. The dimensions for the microstrip line shown in Fig. 5 are: 1) center conductor width = 20 μm; 2) distance to ground plane = 100 μm; 3) thickness = 3 μm; and 4) relative dielectric constant of substrate = 12.9 (appropriate for GaAs). For the normal conductor, the conductivity is given by $\sigma = 4.1 \times 10^7$ S/m (appropriate for gold at room temperature) and for the superconductor, the materials properties are described by a penetration depth of $\lambda = 300$ nm and a normal fluid conductivity of $\sigma_1 = 8.2 \times 10^5$ S/m (these are the same materials parameters for the superconductor used in the calculation of Fig. 2). Fig. 5 also shows the experimental data of Goldfarb and Platzker [15], which are for a gold microstrip line on a GaAs substrate at room temperature. This figure illustrates the agreement of the calculation with experimental data for the normal conductor case and also illustrates the orders of magnitude decrease in loss obtained in planar circuits using superconducting lines compared to normal metal conductors.

V. Validity of the Calculation

The expressions for the conductor loss of superconducting planar elements presented here were derived using the same formalism as for the normal metal case described in [5]. We, therefore, expect the limitations of the superconductor calculations to be similar to those described in [5], which are related to the manner in which the stopping distance was derived. In brief, the calculation of the stopping distance assumes the existence of an isolated edge, thus, it can be expected to break down when the separation between the edges becomes small, as is the case for either a very narrow center conductor or a very small gap spacing between the signal line and ground plane. Note that because the penetration depth of a superconductor is independent of frequency, the calculation for the loss of superconducting lines may be valid to arbitrarily low frequencies, where the skin depth of normal metal conductors approaches the dimensions of the transmission line, violating the assumption of isolated edges. Also, the results of this calculation are easily extended to superconductors with arbitrarily shaped edges, although only the 90° edge profile has been considered here.

One complication of applying this calculation to superconducting materials is the fact that two material parameters need to be specified in order to determine the stopping distance Δ from Fig. 1 (in contrast to the case of normal metal conductors, which require only one material parameter). This means that instead of simply looking up the value for Δ in a table, it may be necessary to search a two-dimensional parameter space for the value of Δ given values for λ and $\delta_{\rm nf}$. This is complicated by the nonmonotonic nature of t/Δ as a function of $t/2\delta_{\rm nf}$ or $t/2\lambda$. However, for the practical examples given above, the values of $t/2\delta_{\rm nf}$ range from 4.6×10^{-4} to 6.3×10^{-3}, showing that, for most superconducting applications, we can in practice make use of the $t/2\delta_{\rm nf} \rightarrow 0$ limit and use just one of the curves shown in Fig. 1.

VI. Conclusions

In summary, we have presented closed-form expressions for the attenuation constant due to conductor loss for superconducting CPW and microstrip lines. These expressions are based on a calculation of the stopping distance Δ, which is a function of the strip thickness t, normal-fluid skin depth $\delta_{\rm nf}$, and London penetration depth λ. Universal curves for Δ have been presented and are used in (2) and (5) to determine the attenuation constant for arbitrary CPW or microstrip geometries. Unlike other quasi-analytical results found in the literature, the expressions presented here are valid for arbitrary conductor thickness. Comparisons to both experimental results and to full numerical techniques found in the literature show very good agreement.

Acknowledgment

The authors acknowledge J. A. Beall, R. H. Ono, L. R. Vale, and D. A. Rudman for experimental assistance, and J. Claassen for performing the penetration depth measurements.

References

[1] Z.-Y. Shen, *High-Temperature Superconducting Microwave Circuits*. Norwood, MA: Artech House, 1994, pp. 103–143.
[2] L. Lewin, "A method of avoiding the edge current divergence in perturbation loss calculations," *IEEE Trans. Microwave Theory Tech.*, vol. MTT-32, pp. 717–719, July 1984.
[3] L. A. Vainshtein and S. M. Zhurav, "Strong skin effect at the edges of metal plates," *Sov. Tech. Phys. Lett.*, vol. 12, no. 6, pp. 298–299, 1986.
[4] C. L. Holloway and E. F. Kuester, "Edge shape effects and quasiclosed form expression for the conductor loss of microstrip lines," *Radio Sci.*, vol. 29, no. 3, pp. 539–559, 1994.
[5] ——, "A quasi-closed form expression for the conductor loss of CPW lines, with an investigation of edge shape effects," *IEEE Trans. Microwave Theory Tech.*, vol. 32, pp. 2695–2701, July 1995.
[6] Z.-Y. Shen, *High-Temperature Superconducting Microwave Circuits*. Norwood, MA: Artech House, 1994, pp. 76–85.
[7] C. L. Holloway and G. A. Hufford, "Internal inductance and conductor loss associated with the ground plane of a microstrip line," *IEEE Trans. Electomag. Compat.*, vol. 39, pp. 73–78, Feb. 1997.
[8] W. Heinrich, "Mode-matching approach for superconducting planar transmission lines including finite conductor thickness," *IEEE Microwave Guided Wave Lett.*, vol. 1, pp. 294–296, Oct. 1991.

[9] F. J. B. Stork, J. A. Beall, A. Roshko, D. C. DeGroot, D. A. Rudman, R. H. Ono, and J. Krupka, "Surface resistance and morphology of YBCO films as a function of thickness," *IEEE Trans. Appl. Superconduct.*, vol. 7, pp. 1921–1924, June 1997.
[10] J. C. Booth, J. A. Beall, D. C. DeGroot, D. A. Rudman, R. H. Ono, J. R. Miller, M. L. Chen, S. H. Hong, and Q. Y. Ma, "Microwave characterization of coplanar waveguide transmission lines fabricated by ion implantation patterning of $YBa_2Cu_3O_{7-\delta}$," *IEEE Trans. Appl. Superconductivity*, vol. 7, pp. 2780–2783, June 1997.
[11] R. B. Marks, "A multiline method of network analyzer calibration," *IEEE Trans. Microwave Theory Tech.*, vol. 39, pp. 1205–1215, July 1991.
[12] J. H. Claassen, M. E. Reeves, and R. J. Soulen, Jr., "A contactless method for measurement of the critical current density and critical temperature of superconducting films," *Rev. Sci. Instrum.*, vol. 62, pp. 996–1004, 1991.
[13] J. H. Claassen, private communication.
[14] D. M. Sheen, S. M. Ali, D. E. Oates, R. S. Withers, and J. A. Kong, "Current distribution, resistance, and inductance for superconducting strip transmission lines," *IEEE Trans. Appl. Superconduct.*, vol. 1, pp. 108–115, June 1993.
[15] M. E. Goldfarb and A. Platzker, "Loss in GaAs microstrips," *IEEE Trans. Microwave Theory Tech.*, vol. 38, pp. 1957–1963, Dec. 1990.

James C. Booth (M'99) received the B.A. degree from the University of Virginia, Charlottesville, in 1989, and the Ph.D. degree from the University of Maryland at College Park, in 1996.

Since 1996, he has been a Physicist in the Electromagnetic Technology Division, National Institute of Standards and Technology, where he began as an NRC Post-Doctoral Research Associate (1996–1998) and is currently a Staff Scientist. As part of the high T_c electronics project at NIST, he is currently involved in the study of the properties of thin-film materials (including high-T_c superconductors) for electronic applications at microwave frequencies.

Christopher L. Holloway (S'86–M'92) was born in Chattanooga, TN, on March 26, 1962. He received the B.S. degree from the University of Tennessee at Chattanooga in 1986, and the M.S. and Ph.D. degrees from the University of Colorado at Boulder in 1988 and 1992, respectively, both in electrical engineering.

During 1992, he was a Research Scientist with Electro Magnetic Applications, Inc., Lakewood, CO, where his responsibilities included theoretical analysis and finite-difference time-domain modeling of various electromagnetic problems. From the fall of 1992 to 1994, he was with the National Center for Atmospheric Research (NCAR), Boulder, CO, where his duties included wave propagation modeling, signal-processing studies, and radar systems design. Since 1994, he has been with the Institute for Telecommunication Sciences (ITS), U.S. Department of Commerce, Boulder, CO, where he is involved in wave propagation studies. He is also on the Graduate Faculty, University of Colorado at Boulder. His research interests include electromagnetic-field theory, wave propagation, guided-wave structures, remote sensing, numerical methods, and electromagnetic compatibility (EMC)/electromagnetic interference (EMI) issues.

Dr. Holloway is a member of Commission A of the International Union of Radio Science. He is currently an Associate Editor on propagation for the IEEE TRANSACTIONS ON ELECTROMAGNETIC COMPATIBILITY.